Structural properties of NaV_2O_5 under high pressure

I. Loa, K. Syassen, and R. K. Kremer
Max-Planck-Institut für Festkörperforschung, Heisenbergstraße 1, D-70569 Stuttgart, Germany

U. Schwarz
Max-Planck-Institut für Chemische Physik fester Stoffe, Pirnaer Landstraße 176, D-01257 Dresden, Germany

M. Hanfland
European Synchrotron Radiation Facility, Boîte Postale 220, F-38043 Grenoble, France

(Received 8 February 1999)

We have investigated the structural properties of NaV_2O_5 under hydrostatic pressure up to 38 GPa at ambient temperature by high-resolution angle-dispersive x-ray powder diffraction. The compression is highly anisotropic with the *c* direction being the soft axis. The pressure dependences of all three axes exhibit pronounced nonlinearities including negative compressibility for the *a* and *b* axes. A reversible structural phase transition towards a pseudotetragonal monoclinic phase starts near 25 GPa and is completed at 35 GPa. Full-profile refinements of the diffraction data provide the internal structural parameters for the low-pressure phase, showing that the structure evolves from a pyramidal towards an octahedral coordination of the vanadium ions. [S0163-1829(99)50334-2]

Sodium vanadate α'-NaV_2O_5 was proposed to represent the second inorganic compound that undergoes a spin-Peierls (SP) phase transition.[1] Magnetic-susceptibility measurements[1] reveal typical features of a SP system: At high temperature the susceptibility as a function of temperature is well described by the Bonner-Fisher model[2] of a one-dimensional antiferromagnetic spin $S=1/2$ Heisenberg chain.[1,3] At a temperature of $T\approx 34$ K, the magnetic susceptibility of α'-NaV_2O_5 drops rapidly, indicating a transition to a nonmagnetic spin-singlet ground state. The opening of a gap in the magnetic excitation spectrum and the lattice dimerization accompanying the transition were evidenced by inelastic neutron scattering and by x-ray and neutron diffraction, respectively.[4,5]

The crystal structure of α'-NaV_2O_5 is shown in Fig. 1. Double chains of edge-sharing distorted VO_5 square pyramids are running along the *b* direction. The chains are corner linked within the *ab* layers. Sodium is intercalated in between sheets which are stacked along the *c* direction. Recent redeterminations of the crystal structure[6–8] indicate the space group *Pmmn* which implies equivalence of all vanadium sites. In view of an average valence of 4.5 for the V atoms, a formation of $S=1/2$ chains is not obvious. This question triggered an active debate about the microscopic origin of the one-dimensional magnetic properties and the character of the phase transition.[7,9,10] Also, a number of experimental findings (see, e.g., Refs. 4,11–14) are inconsistent with or deviate from the expected behavior of a typical SP system.

We report here an investigation of the structural properties of α'-NaV_2O_5 at high pressures. The study was in part motivated by the inherently close relation between elastic and magnetic properties in SP systems.[15,16] Furthermore, this study addresses the question of the stability of the layered structure of α'-NaV_2O_5 and the pyramidal oxygen coordination of V atoms at high pressure. Our results provide a basis for the interpretation of pressure effects on the physical properties of low-pressure α'-NaV_2O_5 and demonstrate a possible high-pressure phase-transition route of related M_2O_5 compounds (*M* denotes transition metal) and their intercalated variants.

The structural properties of α'-NaV_2O_5 under pressure

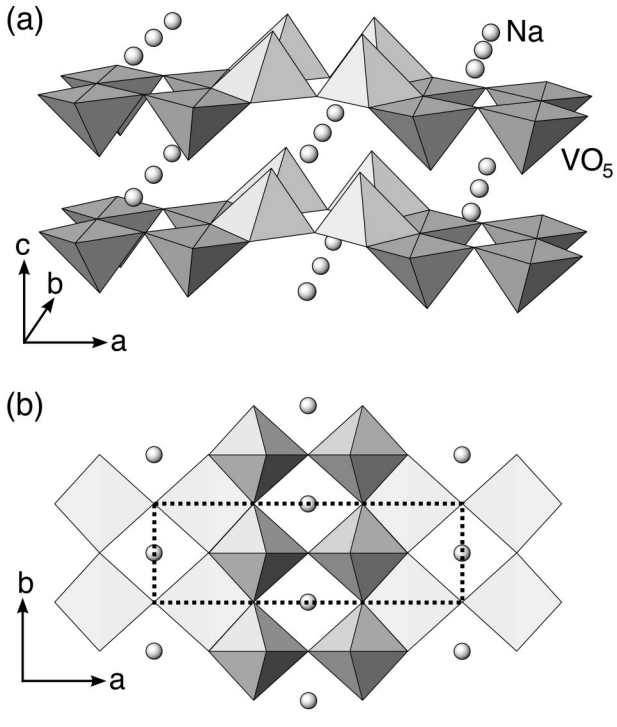

FIG. 1. Crystal structure of α'-NaV_2O_5. (a) Sheets of VO_5 distorted square pyramids are stacked along the *c* direction with intercalated Na. (b) Edge-sharing VO_5 pyramids facing up and down form double chains along the *b* direction. Chains are corner connected within the layers.

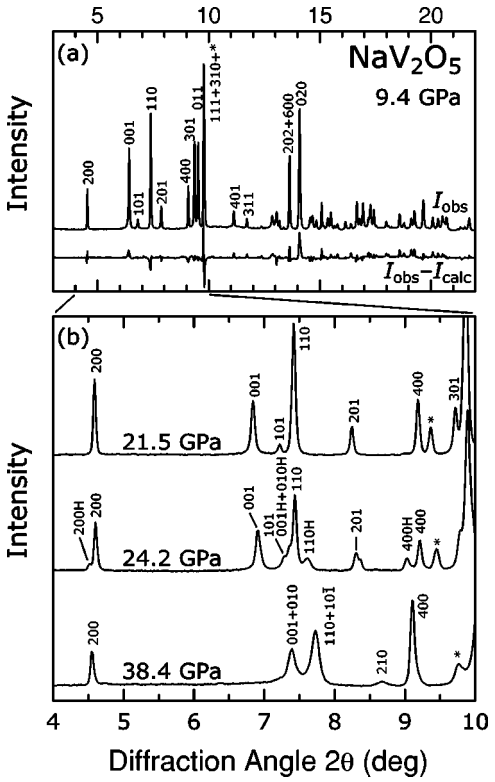

FIG. 2. X-ray powder diffraction patterns of NaV_2O_5 at different pressures ($T=298$ K). Reflections due to solid N_2 are marked by asterisks. (a) Low-pressure phase at 9.4 GPa. The lower curve represents the difference between the observed and calculated profile. (b) Transition from the low- to the high-pressure phase. Peaks marked by an H in the 24-GPa diagram are attributed to the high-pressure phase.

were studied up to 38 GPa by angle-dispersive x-ray powder diffraction at the European Synchrotron Radiation Facility (ESRF Grenoble, beamline ID9). Monochromatic radiation of $\lambda=44.78$ pm was used and the diffraction patterns were recorded on image plates. The images were integrated using FIT2D (Ref. 17) to yield intensity vs 2θ diagrams. For pressure generation a diamond anvil cell (DAC) was used. In order to produce nearly hydrostatic conditions nitrogen was chosen as the pressure medium. The DAC was rocked by $\pm 3°$ to improve the powder averaging. Pressures were measured by the ruby luminescence method using the calibration of Ref. 18.

Crystals of NaV_2O_5 were grown by a self-flux method from a 5:1:1 mixture of $NaVO_3$, V_2O_3, and V_2O_5.[19] The chemical composition of crystals from the same batch was determined as $Na_xV_2O_y$ with $x=0.996(3)$ and $y=5.00(6)$ (cf. sample No. 4 in Ref. 14). The heat capacity $c_p(T)$ showed a single λ-shaped anomaly at $T_{SP}=33.2$ K.[14] The powder sample was prepared by grinding a single crystal at liquid-nitrogen temperature.

Typical diffraction patterns of NaV_2O_5 in the pressure range 0–38 GPa are presented in Fig. 2. Diffraction peaks due to nitrogen, which becomes solid near 2.5 GPa at ambient temperature,[20] are marked by asterisks. From the patterns depicted in Fig. 2(b) it is evident that a structural phase transition starts near 24 GPa.

Up to 19 GPa the diffraction patterns were suitable for full-profile refinements of the lattice parameters as well as the atomic positions. The strongest N_2 diffraction peaks were excluded in the analysis. Refinements were performed using the program CSD.[21] A correction for preferred orientation of the NaV_2O_5 crystallites was taken into account. Typically, the residuals for intensities and the full profile amounted to $R_I=0.15$ and $R_P=0.20$, respectively. The results for the atomic coordinates and lattice parameters are summarized in Table I together with the zero-pressure single-crystal results of Ref. 6 which are consistent with our lowest-pressure values. For pressures higher than 19 GPa the lattice parameters were determined directly from the positions of nonoverlapping diffraction peaks.

Figure 3 illustrates the pressure dependence of the lattice parameters in the low-pressure phase. The compression is highly anisotropic with the soft direction being along the *c* axis. The *c* parameter shortens by 24% at a pressure of 29 GPa, whereas *a* and *b* show an anomalous pressure dependence on a much smaller scale of ~1% (cf. inset of Fig. 3). Under pressure *b increases* by 1% up to 13 GPa and moderately decreases thereafter, adopting the zero-pressure value again at 29 GPa. In contrast, *a* first decreases with increasing

TABLE I. Structural parameters of NaV_2O_5 for various pressures. Zero-pressure data are single-crystal results of von Schnering *et al.* (Ref. 6).

Coord.	0 GPa	0.7 GPa	5.4 GPa	15.5 GPa
z_{Na}	0.3593(5)	0.360(2)	0.356(2)	0.409(3)
x_V	0.09789(4)	0.0983(2)	0.0963(2)	0.0940(3)
z_V	0.10773(3)	0.1111(6)	0.1156(7)	0.0942(10)
x_{O1}	0.1143(2)	0.1116(7)	0.1099(7)	0.0940(9)
z_{O1}	0.4422(5)	0.458(2)	0.484(2)	0.543(4)
x_{O2}	−0.0729(2)	−0.0741(7)	−0.0785(7)	−0.0824(9)
z_{O2}	0.0121(5)	0.014(2)	0.008(2)	−0.041(4)
z_{O3}	−0.0189(5)	−0.013(3)	0.021(3)	0.058(6)
a (Å)	11.311(2)	11.2966(4)	11.2877(4)	11.2525(5)
b (Å)	3.6105(6)	3.6145(1)	3.6322(1)	3.6512(2)
c (Å)	4.800(1)	4.6841(1)	4.2388(2)	3.8506(2)

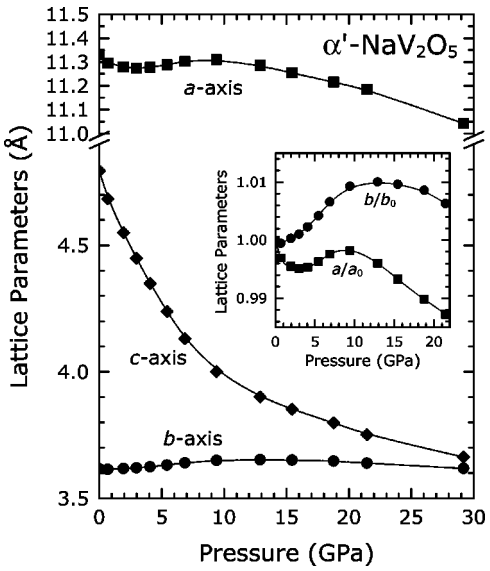

FIG. 3. Lattice parameters of α'-NaV_2O_5 (low-pressure phase) as a function of pressure. Solid lines are guides to the eye. The inset depicts the *relative* changes of *a* and *b*.

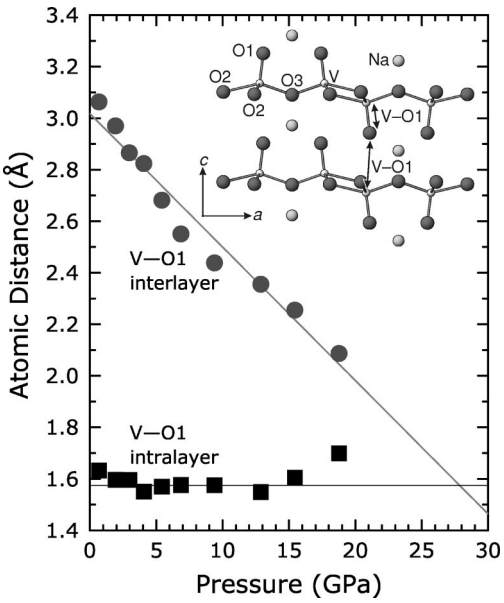

FIG. 5. Pressure dependence of the intra- and interlayer V–O1 distance.

pressure up to 4 GPa, then increases up to 10 GPa, and finally decreases again at higher pressure values.

From the lattice parameter data we obtain the pressure dependence of the cell volume shown in Fig. 4. The $V(P)$ dependence is well described by a Birch relation[22]

$$P(V)=\tfrac{3}{2}B_0(v^7-v^5)[1-\tfrac{3}{4}(B'-4)(1-v^2)], \qquad (1)$$

where $v=(V/V_0)^{-1/3}$. The volume at zero pressure was set to $V_0=196.2$ Å^3 in accordance with an independent structure determination.[14] Fitting Eq. (1) to the experimental data yields the bulk modulus $B_0=24\pm3$ GPa and a pressure derivative $B'=12\pm3$ at zero pressure. The large value of B' (compared to typical values of $B'\approx4$–6 for three-dimensionally connected crystals) is characteristic for materials with strongly anisotropic compression properties such as the archetypical graphite[23] or the SP compound $CuGeO_3$.[24]

The difference between the *b* and *c* lattice parameters is reduced significantly under pressure, which implies a continuous change from a square pyramidal towards a distorted octahedral coordination for V. In fact, from the refinement of the positional parameters we infer that up to 20 GPa the main effect of pressure is to move the apex oxygens (O1) into a more symmetrical position in between V ions belonging to neighboring layers. This is illustrated in Fig. 5 which compares the distance between the V atom and the apex oxygen within the pyramid with that for the corresponding oxygen ion in the adjacent layer. While the intrapyramid distance is hardly affected, the interlayer distance decreases strongly under pressure. An increased layer interaction becomes evident also from our first Raman experiments which show a pronounced softening of the V–O1 phonon (970 cm^{-1} at ambient conditions[25]). These experiments also reveal an anomalous continuous change of phonon frequencies for pressures below 10 GPa that is closely related to the anomalous behavior of the *a* and *b* axes. The refined positional parameters suggest that these effects are caused by a small tilting of the VO_5 pyramids at pressures around 5 GPa. The tilting occurs such that the small buckling in the O2-O3 atom planes is diminished and the O1 atoms give space to the Na ions.

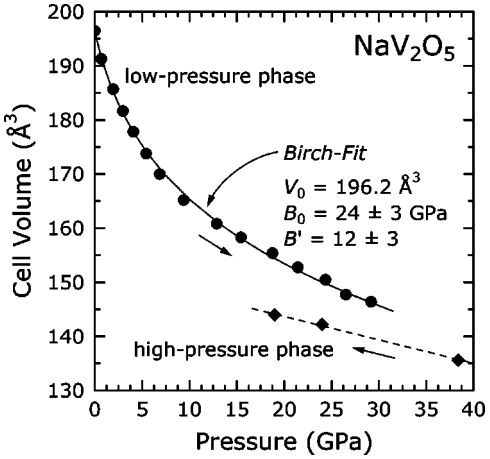

FIG. 4. Unit-cell volume of NaV_2O_5 as a function of pressure. The solid line refers to a fitted Birch relation (1).

In the pressure range around 25–30 GPa, where according to an extrapolation of the data in Fig. 5 the V–O1–V chains along *c* would become almost uniformly spaced, a new structural phase evolves. This transition is sluggish and is completed only at a pressure of ~35 GPa. Near the onset of the phase transition (24 GPa) two weak additional peaks were seen [$2\Theta=7.36°$ and $2\Theta=8.37°$, not labeled in Fig. 2(b)], which cannot be attributed to the low- or high-pressure phase and which indicate the possible existence of an intermediate phase or a lattice modulation. Upon reduction of the pressure from 38 GPa, the ambient-pressure phase started to reappear at 20 GPa, and at zero pressure this phase is fully recovered.

Diffraction patterns of the high-pressure phase at 38, 24, and 19 GPa can be indexed consistently (using ~20 reflections) with a monoclinic cell.[26] The unit cell of the high-pressure phase is close to tetragonal, i.e., *b* and *c* differ by only 0.01 Å and the monoclinic angle is close to $\beta=90°$.

The cell volume changes discontinuously across the phase transition as is shown in Fig. 4. The small volume difference [$\Delta V/V=-5(1)\%$ at 30 GPa] implies that the number of atoms per cell remains unchanged. Furthermore, the unit-cell parameters of the low- and high-pressure phase are closely related. This suggests an interpretation of the structural transition, where the orthorhombic lattice of the low-pressure phase expands along the *a* direction, while the two other axes contract. The overall metrical changes are small. This indicates that the basic structural motif, i.e., edge- and corner-linked distorted octahedra within the *ab* planes with polyhedra in neighboring layers sharing corners, is preserved. The ratio $a/3c$ is 1.084. Thus, the distortion of octahedra consists mainly of an elongation along the *a* direction. The octahedral voids in the proposed high-pressure structure can accommodate the Na ions.

Several phases of Nb_2O_5 show a very similar arrangement of distorted octahedra.[27,28] Moreover, the axial ratio of the tetragonal *P* phase of Nb_2O_5 is surprisingly close to that given above, except for a factor of 2 difference due to the formation of a superlattice in *P*-Nb_2O_5 along the tetragonal *c* axis ($c/6a=1.085$). Similar to interpretations of the *P* and *R* phases of Nb_2O_5, the high-pressure phase of NaV_2O_5 can be viewed as a distortion of the *idealized* V_2O_5 structure.[27] NaV_2O_5 approaches such a highly symmetric three-dimensional structure, but in addition to the nonideal axial ratio there is a small monoclinic distortion.

Nakao *et al.*[29] recently reported the observation of a phase transition in NaV_2O_5 at a pressure as low as 13 GPa. In none of our diffraction experiments under quasihydrostatic conditions (N_2 medium) could we find an indication for a phase transition at such a low pressure. Only when using a less hydrostatic pressure medium (CsCl) our Raman and optical reflectivity experiments indicated a pressure-induced transition starting at 18 GPa. This transition involves substantial changes of the vibrational and electronic properties. It remains to be investigated if the transition induced under nonhydostatic conditions is identical to the structural change reported here.

In summary, the compression of α'-NaV_2O_5 is highly anisotropic with the *c* axis being the soft direction. Furthermore, the compression is nonlinear for all axes with negative compressibility of the *a* and *b* axes. With increasing pressure, the coordination of the V atoms evolves from square pyramidal towards a distorted octahedral one. This process is intercepted by a reversible structural phase transition at 25–35 GPa. The structure of the high-pressure phase is proposed to be a distorted monoclinic variant of the ''idealized'' V_2O_5 structure. It is also a possible candidate for a high-pressure phase of V_2O_5 which was recently detected by Raman spectroscopy.[30]

Part of this work was supported by GIF Grant No. I0428-086.10/95.

[1] M. Isobe and Y. Ueda, J. Phys. Soc. Jpn. **65**, 1178 (1996).
[2] J. C. Bonner and M. E. Fisher, Phys. Rev. **135**, A640 (1964).
[3] A. Carpy *et al.*, Acta Crystallogr., Sect. B: Struct. Crystallogr. Cryst. Chem. **31**, 1481 (1975).
[4] Y. Fujii *et al.*, J. Phys. Soc. Jpn. **66**, 326 (1997).
[5] T. Chatterji *et al.*, Solid State Commun. **108**, 23 (1998).
[6] H. G. von Schnering *et al.*, Z. Kristallogr. **213**, 246 (1998).
[7] H. Smolinski *et al.*, Phys. Rev. Lett. **80**, 5164 (1998).
[8] A. Meetsma *et al.*, Acta Crystallogr., Sect. C: Cryst. Struct. Commun. **54**, 1558 (1998).
[9] P. Thalmeier and P. Fulde, Europhys. Lett. **44**, 242 (1998).
[10] P. Horsch and F. Mack, Eur. Phys. J. B **5**, 367 (1998).
[11] A. N. Vasil'ev, A. I. Smirnov, M. Isobe, and Y. Ueda, Phys. Rev. B **56**, 5065 (1997).
[12] T. Ohama, M. Isobe, H. Yasuoka, and Y. Ueda, J. Phys. Soc. Jpn. **66**, 545 (1997).
[13] M. Köppen *et al.*, Phys. Rev. B **57**, 8466 (1998).
[14] W. Schnelle, Y. Grin, and R. K. Kremer, Phys. Rev. B **59**, 73 (1999).
[15] J. W. Bray, L. V. Interrante, I. S. Jacobs, and J. C. Bonner, in *Extended Linear Chain Compounds*, edited by J. C. Miller (Plenum Press, New York, 1983), Vol. 3, pp. 353–415.
[16] A. I. Buzdin and L. N. Bulaevskiĭ, Usp. Fiz. Nauk **131**, 495 (1980) [Sov. Phys. Usp. **23**, 409 (1980)].
[17] A. Hammersley, computer program FIT2D, ESRF, Grenoble, 1998.
[18] H. K. Mao, J. Xu, and P. M. Bell, J. Geophys. Res. **91**, 4673 (1986).
[19] M. Ueda, C. Kagami, and Y. Ueda, J. Cryst. Growth **181**, 314 (1997).
[20] R. L. Mills, B. Ollinger, and D. T. Cromer, J. Chem. Phys. **84**, 2837 (1986).
[21] L. G. Akselrud, Yu. Grin, V. K. Pecharsky, P. Yu. Zavaliy, and V. S. Fundamenskiy, computer program CSD 4.1, STOE & Cie, Darmstadt, Germany, 1992.
[22] F. Birch, J. Geophys. Res. **83**, 1257 (1978).
[23] M. Hanfland, H. Beister, and K. Syassen, Phys. Rev. B **39**, 12 598 (1989).
[24] S. Bräuninger *et al.*, Phys. Rev. B **56**, R11 357 (1997).
[25] Z. V. Popović *et al.*, J. Phys.: Condens. Matter **10**, L513 (1998).
[26] We determined the following sets of lattice parameters for the high-pressure phase of NaV_2O_5 at the given pressures. 38.4 GPa: $a=11.29$ Å, $b=3.47$ Å, $c=3.46$ Å, and $\beta=92.0°$; 24.0 GPa: $a=11.46$ Å, $b=3.52$ Å, $c=3.53$ Å, and $\beta=91.8°$; 19.0 GPa: $a=11.48$ Å, $b=3.55$ Å, $c=3.54$ Å, and $\beta=92.4°$.
[27] R. Gruehn, J. Less-Common Met. **11**, 119 (1966), and references therein.
[28] *Physics of Non-tetrahedrally Bonded Binary Compounds III*, edited by O. Madelung Landolt-Börnstein, New Series, Group 3, Vol. 17, Pt. g (Springer-Verlag, Berlin, 1984).
[29] H. Nakao *et al.*, Physica B **241-243**, 534 (1998).
[30] A. Grzechnik, Chem. Mater. **10**, 2502 (1998).